JOURNAL OF CATALYSIS **177,** 11–21 (1998)
ARTICLE NO. CA982087

Titanium-Cobalt Cluster of Cluster-Based Catalysts for the Selective Hydrogenation of α,β-Unsaturated Aldehydes

Michael C. LaNeve,* Xinjian Lei,† Thomas P. Fehlner,† and Eduardo E. Wolf*,[1]

*Departments of Chemical Engineering and †Chemistry and Biochemistry, University of Notre Dame, Notre Dame, Indiana 46556

Received July 29, 1997; revised March 20, 1998; accepted March 25, 1998

The characterization and catalytic properties of a new molecular cluster precursor, $Ti_4O_4[OCH(CH_3)_2]_4\{(CO)_9Co_3CCO_2\}_4$, denoted Ti_4Co_{12}, were studied during the vapor phase hydrogenation of 2-butenal to form the thermodynamically less favored product, 2-butenol. Pyrolysis of this precursor yields three active catalytic forms, designated LT-, HT1-, and HT2-. This catalyst shows enhanced thermal stability (up to 400°C) as compared to $M_2\{(CO)_9Co_3CCO_2\}_4$ (where M = Co, Cu, or Mo) and $M_4O\{(CO)_9Co_3CCO_2\}_6$ (where M = Zn or Co), which are stable only to 300°C. It has been found that the HT1-Ti_4Co_{12} structure provides significantly better selectivity to 2-butenol than the HT2-Ti_4Co_{12} structure. *In-situ* **DRIFTS measurements during the decomposition of the precursor indicate the presence of COO^- groups during the formation of the selective HT1-Ti_4Co_{12} form. These groups disappear at higher temperatures when the HT2-Ti_4Co_{12} catalyst is formed. We speculate that these ions are related to the high selectivity of these materials.**

INTRODUCTION

The selective hydrogenation of α,β-unsaturated aldehydes to the corresponding unsaturated alcohols is an important reaction in the production of pharmaceuticals, cosmetics, and perfumes (1, 2). Formation of unsaturated alcohol is a challenging problem in heterogeneous catalysis. Typically, the hydrogenation of α,β-unsaturated aldehydes proceeds with hydrogenation of the C=C bond (3, 4). For the reaction pathway given in Fig. 1, the thermodynamically favored product is the saturated aldehyde, butanal, and the thermodynamically least favored product is the desired product, the unsaturated alcohol, 2-butenol (5). On metal catalysts, the reactivity of an isolated C=C bond is greater than the reactivity of an isolated C=O bond (6, 7). Additionally, it has been found that the reactivity of a C=C bond is greatly enhanced when conjugated with a C=O bond when reacted in a vapor phase catalytic reaction (8). These factors typically lead to a low selectivity of the unsaturated alcohol.

The gas phase catalytic hydrogenation of 2-butenal to form the unsaturated alcohol, 2-butenol, has been the subject of many studies (5, 9–24). The most common methods used to increase the amount of unsaturated alcohol produced include adding promoters (9–14), controlled poisoning (15, 16), or choice of support (5, 17, 18). Deactivation and time-dependent selectivities over extended periods are also observed for this reaction (14, 23).

In an attempt to control the characteristics of the crystallites in a supported catalyst, metal clusters have been used as precursors of the active metal (25–27). Industrially, supported heterogeneous metal catalysts are often used because of their high activity and because downstream separation of the catalyst and the chemicals involved in the reaction are not needed (27). Since most active metals are usually expensive (i.e., Pt, Pd, etc.), they are typically impreganted on a porous support in low concentration to allow as much of the metal as possible to be exposed on the surface and to participate in the chemical reaction. Because the supports used have nonuniform surfaces and the metal particles are also nonuniform and too small in size to be characterized precisely, the structures of these catalysts are not well understood (26). This lack of understanding of the structure of the catalysts makes difficult the rational design of catalysts which have the desired catalytic properties for a particular reaction. To partially circumvent these problems, the use of metal clusters as catalyst precursors has become more common in the past decade. For heterogeneous reactions the metal clusters typically have to be used in a supported form. Many reactions have been studied using metal cluster catalysts, including isomerizations, reductions of multiple bonds, hydroformylation, Fischer–Tropsch synthesis, and the water–gas shift reaction (28). The ability to prepare and characterize the metal clusters makes them well suited for catalytic studies.

Recently, Nashner *et al.* have reported the use of molecular carbonyl clusters as precursors for supported metal catalysts (25). Their procedure results in active metal particles with a narrow size distribution which are of nanoparticle size. Thus, using molecular carbonyl clusters as precursor for metal catalysts provides a method to control the synthesis of the metal catalyst.

0021-9517/98 $25.00

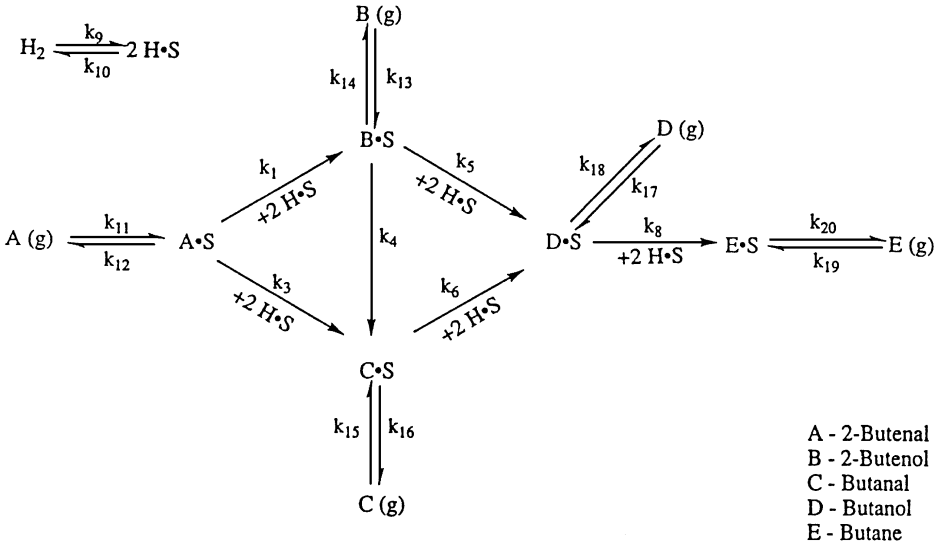

FIG. 1. Reaction pathway for kinetic model.

Previous work in our group has shown that it is possible to use transition metal clusters as a replacement for methyl groups in a metal acetate (29–31). The molecules formed by this procedure consist of a metal acetate core cluster surrounded by the transition metal clusters (a cluster of clusters). It is possible to make systematic changes in both the geometry and metal composition of the clusters to see how these changes affect their catalytic properties.

A novel feature of the cluster of clusters compounds is that the precursors lead to the formation of high surface area metal catalysts. Therefore the resulting materials are self-supported and there is no need of using a high area support. Previously, we have used these catalysts for the selective hydrogenation of 1,3-butadiene and 2-butenal (32–35). Coordination compounds with complex cluster substituents have been found to be stable precursors for the formation of selective catalysts for the hydrogenation of α,β-unsaturated aldehydes. Previous work has focused on studying the catalytic properties of $M_2\{(CO)_9Co_3CCO_2\}_4$ (where M = Co, Cu, or Mo) and $M_4O\{(CO)_9Co_3CCO_2\}_6$ (where M = Zn or Co). The precursor materials, before pyrolysis, were found to have low surface area and no catalytic activity. However, pyrolysis of these materials results in the loss of carbonyl and carboxylate ligands, exposing the metal atoms and making the material a selective catalyst for the hydrogenation of compounds with conjugated double bonds. Moreover, after decomposition of the precursors, these materials have BET areas in the range of 50–200 m^2/g.

In this paper, we report detailed kinetics and characterization results of the gas phase hydrogenation of 2-butenal using a newly synthesized cluster of clusters compound, $Ti_4O_4(OCH(CH_3)_2)_4\{(CO)_9Co_3CCO_2\}_4$ (36), denoted Ti_4Co_{12} (see Fig. 2).

EXPERIMENTAL

Catalyst Preparation

The catalyst precursor is synthesized by reaction of $(CO)_9Co_3CCO_2H$ and $Ti(OCH(CH_3)_2)_4$ under a nitrogen atmosphere. The resulting molecule contains a TiO_2 core surrounded by four tricobalt clusters. This is a form of a nano-supported molecule, where each TiO_2 core acts as a support of the tricobalt clusters surrounding it. The strength of the Ti–O bond results in catalysts with good thermal stability. The precursor itself shows no catalytic activity, and thermal activation is required to yield active materials. Activation is performed in a hydrogen atmosphere. Activation of the precursor is performed *in situ*, prior to the activity measurements. Three activation temperatures

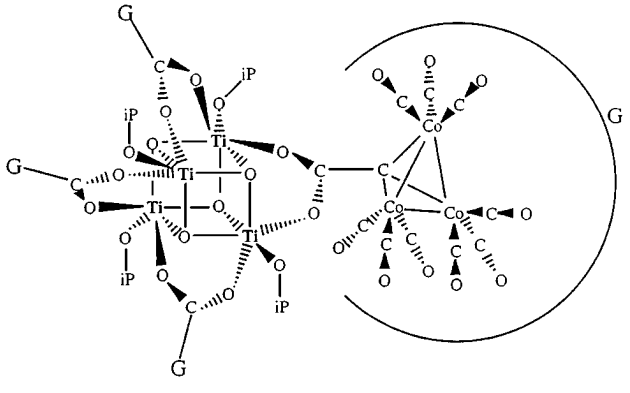

FIG. 2. Structure of the $Ti_4O_4(OCH(CH_3)_2)_4\{(CO)_9Co_3CCO_2\}_4$ precursor.

are used, 393, 493, and 673 K. The activation period lasts 2 h.

Thermogravimetric Analysis

The metal cluster weight loss taking place as a function of temperature was found using a Cahn RG Electrobalance. The electrobalance settings used were a mass dial range of 10 and a recorder range of 1. Typically, a 20-mg sample was used, and its temperature was increased either linearly from 300 to 673 K or in steps up to 673 K in flowing hydrogen at 100 mL/min. All the gases used were ultra-high purity. In addition, oxygen and water traps were incorporated into the hydrogen line. A small flow of argon was used to purge the electronics of the electrobalance. The weight loss was recorded as a function of temperature.

Temperature Programmed Decomposition-Mass Spectroscopy

Mass spectrometric analyses were performed with a UT-100C Precision Mass Analyzer equipped with a fast response continuous inlet system to determine the nature of the species which evolve during thermal decomposition of the precursor. The mass spectrometer was operated in the 10^{-11} amp range with a filament current of 0.30 mA. Typically, a 10-mg sample was used, and its temperature was increased linearly from 300 to 673 K over a 45-min period in 100 mL/min of flowing helium. SpectraSoft™ software was used to record the results.

Diffuse Reflectance Infrared Spectroscopy (DRIFTS)

Information of the structure of the cluster of cluster catalysts during activation was gathered using *in-situ* diffuse reflectance infrared spectroscopy (DRIFTS). These experiments were performed in a DRIFTS reaction cell (Harrick Scientific Corporation) placed in an FTIR spectrometer (Mattson Instruments, Galaxy Model 6020). All infrared spectra were recorded in Kubelka-Munk units and were taken using 416 scans at a resolution of 4 cm^{-1}.

For these experiments, 5 mg of the sample and 85 mg of KBr were ground separately and then mixed. The resulting powder was then placed in the sample cup located in the DRIFTS reaction cell. The upper surface of the solid was made level and flush with the top of the sample cup by dragging a spatula across the top of the sample cup. Flowing hydrogen (50 mL/min) was used during activation and traveled up through the sample bed. The DRIFTS reaction cell included a heating element and thermocouple which were connected to an Eurotherm Model 808 Temperature Controller. This allowed for heating of the sample to 573 K.

Surface Area Determination

The BET surface area of the materials after pyrolysis was obtained using a Quantachrome Monosorp MS 16 instrument using the continuous flow-adsorption method at 77 K (cooled by liquid nitrogen). The adsorbate was a 30% nitrogen in helium mixture. The BET surface area was automatically calculated by the instrument based on the BET adsorption isotherm.

Catalytic Activity

The hydrogenation of 2-butenal (99+%, Aldrich Chemical Company, Inc.) was studied in a quartz flow microreactor with an internal diameter of 4 mm and a length of 35 cm. The catalyst bed height was confined by quartz wool plugs. The catalyst was activated under hydrogen in the temperature range of 393–673 K. During activity measurements the total hydrogen flow was varied. This was done to provide a range of residence times to facilitate kinetic modeling of the reaction. Traps were incorporated into the hydrogen and helium lines to remove any oxygen or water present. The hydrogen and helium flow rates were controlled by electronic flow controllers (5850-E, Brooks Instruments) and the system was automated and computer controlled (Lab VIEW2, National Instruments). The entering gas stream was bubbled through 2-butenal kept at 273 K by an ice bath.

To prevent condensation, the lines downstream from the reactor were heated. The reactor effluent could either be sent to a gas chromatograph or a mass spectrometer. During the activity studies, the reactor effluent was analyzed by a Varian Model 3700 Gas Chromatoghaph with an FID detector. The FID temperature was kept at 473 K. A 10% Carbowax 20M on Chromosorb W-HP 80/100 mesh 50″-long packed column (Alltech) at 363 K was used to separate the effluents, which were butane, 1-butanal, 2-butenal, 1-butanol, and 2-butenol. Peak areas were calculated by a Hewlett Packard 3395 Integrator.

RESULTS AND DISCUSSION

Thermogravimetric Analysis

Thermogravimetric analysis of the Ti_4Co_{12} cluster of cluster precursor was performed to determine the temperatures at which weight losses occur. Initially, the thermogravimetric analysis was completed with a linear temperature ramp from 298 to 673 K over 3 h. Ti_4Co_{12} showed weight losses at three distinct temperatures (Fig. 3a). After determining the temperature ranges where the weight losses occur, the temperature ramp was changed so that the temperature was increased in steps with the temperature for each step determined from the linear temperature ramp experiment. The solid was left at the desired temperature until an equilibrium in weight loss was reached. The results for this experiment can be found in Fig. 3b. As it can be seen, three separate weight losses occur to form three distinct, stable structures. The first structure, designated LT, occurs

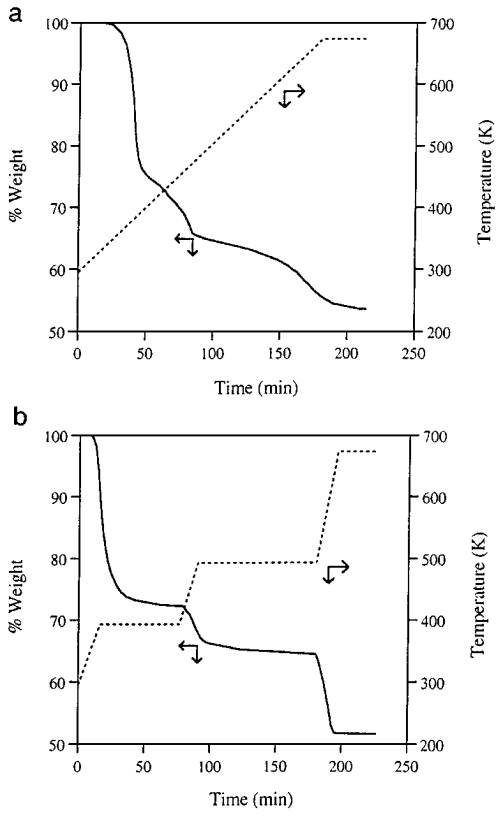

FIG. 3. TGA results for Ti_4Co_{12} with (a) a linear temperature profile and (b) a step temperature profile.

at 393 K and corresponds to a weight loss of 27.7%. The second structure, designated HT1, occurs at 493 K and corresponds to an additional weight loss of 7.8%. The third structure, designated HT2, occurs at 673 K and corresponds to an additional weight loss of 12.8%.

The total weight loss observed for the Ti_4Co_{12} compound is 48.3%. The theoretical percentage weight loss that corresponds to the loss of all CO ligands, CO_2 ligands, and isopropyl groups is 55.8%. From this it seems likely that some of the carbon and/or oxygen atoms from these groups still remain in the final structure after all the weight loss has occurred. The residual carbon and/or oxygen atoms in the structure could provide the framework for the high surface area structures formed.

Temperature Programmed Decomposition-Mass Spectroscopy

To determine the nature of the species evolving during decomposition of the precursor, temperature programmed decomposition experiments monitored by mass spectroscopy were performed. The species evolved during pyrolysis have m/e signals assigned to CO, CO_2, CH_4, C_2, and C_3 hydrocarbons and CH_3CH_2CHO. The CO molecules evolve from the external carbonyl ligands in the precursor, the CO_2 molecules from the carboxylate ligands, the CH_4, C_2, and C_3 molecules from the isopropyl groups, and the CH_3CH_2CHO from a reaction between a C_2 group from the isopropyl group and a CO from a carbonyl ligand.

As can be seen from Fig. 4, CO, CO_2, CH_4, C_2, and C_3 hydrocarbons, and CH_3CH_2CHO begin evolving at approximately 373 K, corresponding to the formation of the LT structure. The formation of the HT1 structure begins at approximately 423 K and also has CO, CO_2, CH_4, C_2, and C_3 hydrocarbons, and CH_3CH_2CHO evolving. Formation of the HT2 structure begins occurring at approximately 600 K with the evolution of CO_2 and CH_4. The signals for the species from the carbonyl ligands (CO and CH_3CH_2CHO) and the signals for the species from the isopropyl groups (CH_4, C_2, and C_3 hydrocarbons, and CH_3CH_2CHO) are more intense than the signal from the carboxylate groups. This agrees with the stoichiometry of the precursor, where the carbonyl ligands and isopropyl groups are more numerous than the carboxylate ligands.

A difference is seen when comparing these results to the previous results of cluster of cluster compounds having M_2Co_{12} and M_4Co_{18} structures. For those geometries the carbonyl groups evolved first, followed by evolution of the carboxylate groups (35). The LT structure of these materials was formed through the evolution of mainly carbonyl groups. Thus, in that case only the outer Co atoms

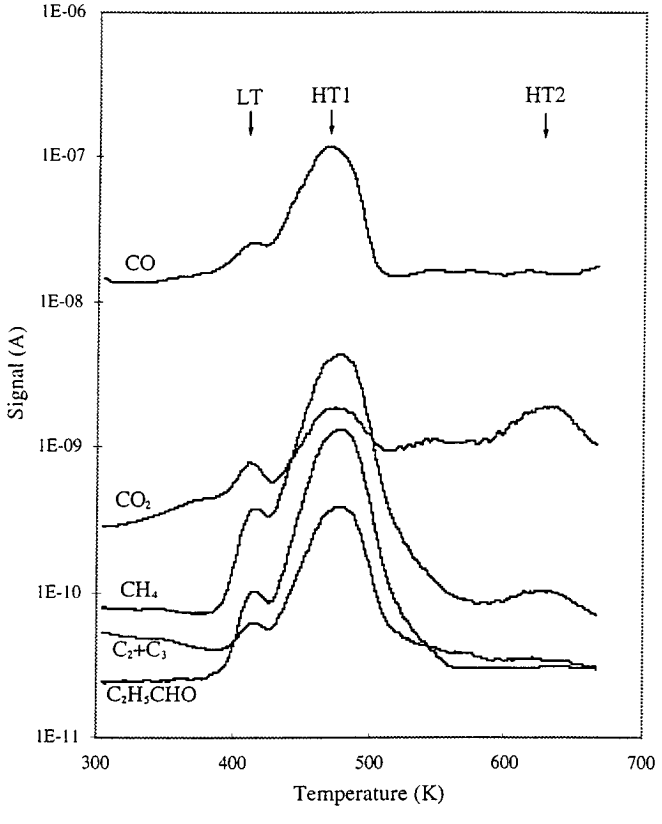

FIG. 4. Temperature programmed decomposition-mass spectroscopy during decomposition of Ti_4Co_{12}.

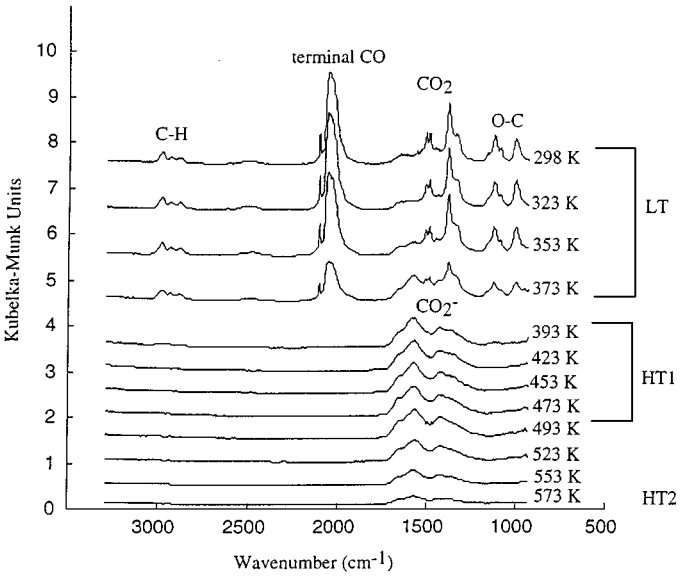

FIG. 5. DRIFTS during activation of Ti_4Co_{12}.

are affected by the loss of the CO ligands. For the Ti_4Co_{12} compound, however, the evolution of the carbonyl and carboxylate groups occur simultaneously. Hence, there is a more drastic rearrangement at low temperatures for the Ti_4Co_{12} compound, compared to the M_2Co_{12} and M_4Co_{18} compounds.

Diffuse Reflectance Infrared Spectroscopy (DRIFTS)

The infrared spectra during the pyrolysis of Ti_4Co_{12} in hydrogen, recorded *in situ* using DRIFTS can be found in Fig. 5. The spectrum at 298 K is for the Ti_4Co_{12} precursor. The following band assignments can be made: C–H stretch at 3000 to 2900 cm^{-1}, a well-defined band characteristic of the intact $(CO)_9Co_3C$-cluster at 2100 cm^{-1}, the vibrational mode of a terminal carbonyl group at 2050 cm^{-1}, the symmetric and anti-symmetric vibrational modes of the carboxylate ligands at 1500 and 1385 cm^{-1}, and an O–C stretch at 1130 and 1000 cm^{-1}.

As the temperature increases, the intensity of the peaks begins to decrease, starting at 383 K. This corresponds to the temperature where weight loss begins in the thermogravimetric analysis and gases begin to evolve in the mass spectroscopy analysis. It can be seen that the decrease in peak intensities for all of the peaks begin at the same temperature. This agrees with the mass spectroscopy results which show the different gases evolving simultaneously. At 373 K two new peaks at 1570 and 1425 cm^{-1} begin to form. These peaks can be respectively assigned to the anti-symmetric and symmetric stretching regions of ionized carboxylate groups (37). These ionized carboxylate groups (COO^-) form due to the presence of the tricobalt clusters. These peaks disappear at $\approx$573 K, with the formation of the HT2 structure. The elimination of the COO^- band with the formation of the HT2 structure agrees with the mass spectroscopy results which show evolution of CO_2 with the formation of the HT2 structure. While these characterization techniques provide information as to when species evolve and the nature of the species evolving, the actual structures of the LT, HT1, and HT2 catalysts are still unknown.

There is some discrepancy between the temperatures at which bands disappear in the DRIFTS experiments and the temperature at which species evolve from the mass spectroscopy experiments. The difference can be explained by the fact that the temperature probes were located at different points in the TGA and DRIFT cell. In addition, the mass spectroscopy experiments were performed in He as opposed to H_2 in the thermogravimetric analysis and the DRIFTS experiments. All experiments were run under a hydrogen atmosphere; hence we used hydrogen activation to maintain the same atmosphere during reaction. Helium was used only during the mass spectroscopy experiments so the species identified by the mass spec would be those evolved from the precursor and not those that could form from reaction with hydrogen. TGA showed that under both hydrogen and helium atmospheres, the three distinct structures were formed at similar temperatures.

Surface Area Determination

The BET surface area of the $Ti_4O_4[OCH(CH_3)_2]_4\{(CO)_9Co_3CCO_2\}_4$ precursor is small ($\approx$6 m^2/g). However, pyrolysis of this precursor results in porous materials with surface areas between 61 to 84 m^2/g (see Table 1). The BET measurements were performed *in situ*, such that the activated cluster of cluster materials were never exposed to air. The dramatic increase in surface area from the precursor to the LT, HT1, and HT2 structure shows that the evolution of the gases upon pyrolysis results in the formation of a porous structure. This porous structure is probably the result of a network of pores which forms between neighboring molecules when metal–metal bonds formed as ligands are evolved. It is important to note that the HT2-Ti_4Co_{12} structure is still a high surface area structure. Our previous cluster of cluster compounds with M_2Co_{12} and M_4Co_{18}

TABLE 1

BET Areas and Specific Reaction Rates for Ti_4Co_{12} Structures

Structure	BET area m^2/g	Reaction rates[a] moles/hr g	
Ti_4Co_{12} precursor	6	393 K	423 K
LT-Ti_4Co_{12}	61	0.16×10^{-2}	
HT1-Ti_4Co_{12}	75	0.17×10^{-2}	1.4×10^{-2}
HT2-Ti_4Co_{12}	84	1.07×10^{-2}	2.13×10^{-2}

[a] 10 mg of precursor, weight loss %: LT = 27.7, HT1 = 35.5, HT2 = 48.3, 25 cc/min, 1.2% 1-butenal.

geometries, heating above 573 K resulted in the loss of the high surface area structure (38). Thus, the more robust TiO_2 core used in the present work resulted in a more thermally stable structure which retains its high surface area after being heated to at least 673 K.

Catalytic Activity

The reactivities of LT-Ti_4Co_{12}, HT1-Ti_4Co_{12}, and HT2-Ti_4Co_{12} were evaluated using the gas phase hydrogenation of 2-butenal. In all of these experiments 10 mg of the Ti_4Co_{12} precursor were used. The reactant gas consisted of only hydrogen and 2-butenal, with the flow rate varied from 5 to 30 mL/min to allow for a variety of residence times.

All three of these catalysts proved to be effective catalysts for the selective gas phase hydrogenation of 2-butenal to form 2-butenol. However, at the same conversion level, the HT1-Ti_4Co_{12} catalysts provided higher 2-butenol yield than either the LT-Ti_4Co_{12} or the HT2-Ti_4Co_{12} catalysts. Figure 6 shows a comparison of the 2-butenol yields provided by these three catalysts at a reaction temperature of 393 K. This temperature was used so all three catalysts can be compared at the same temperature. This is the maximum temperature at which the LT-Ti_4Co_{12} catalyst can be used. In fact, as can be seen, the 2-butenol yields for LT-Ti_4Co_{12} and HT2-Ti_4Co_{12} fall on nearly identical curves while the yields for HT1-Ti_4Co_{12} are slightly more than twice as great. It is speculated that the reason for the enhanced 2-butenol yields of the HT1-Ti_4Co_{12} catalyst are attributable to the CO_2^- group unique to this structure as identified in the DRIFTS experiments. This charged group would act to increase the polarization of the carbonyl group in 2-butenal which would facilitate hydrogenation there and lead to a relative increase in the amount of 2-butenol formed.

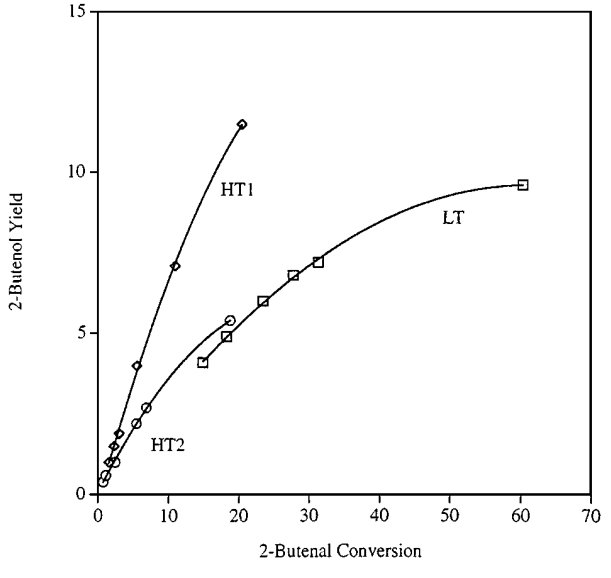

FIG. 6. 2-Butenol yields for LT-, HT1-, and HT2-Ti_4Co_{12} at 393 K.

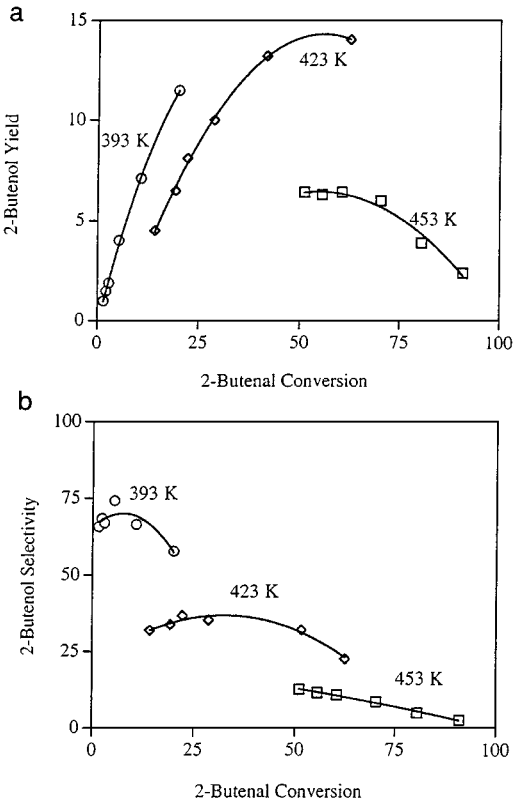

FIG. 7. 2-Butenol (a) yields and (b) selectivities for HT1-Ti_4Co_{12}.

Figure 7a shows the 2-butenol yields of the HT1-Ti_4Co_{12} catalyst at three different temperatures, 393, 423, and 453 K. This graph shows characteristics of a typical yield versus conversion graph. The 2-butenol yield is defined here as the product of the 2-butenal conversion and the 2-butenol selectivity. Typically, a graph of yield versus conversion is a continuous curve. However, since the results shown in Fig. 7a are for three different temperatures, discontinuities exist in the curve. At the same conversion levels higher 2-butenol yields are achieved at lower temperatures. This means that at a given conversion, the selectivity of 2-butenol increases with decreasing temperature. From this it is expected that the activation energy for the formation of 2-butenol is lower than the activation energy for the formation of butanal. Indeed, as will be seen through kinetic modeling of this reaction, this appears to be the case.

As can be seen in Fig. 7a, the maximum yield achieved for these catalysts is 14.0%. The highest steady state, 2-butenol yield reported in the literature outside our group for the gas phase hydrogenation of 2-butenal is 10.0% (14). Figure 7b shows the selectivities obtained for the HT1-catalyst. The highest selectivity achieved is approximately 74%. This also compares very favorably with other's 2-butenol selectivities reported in the literature, where the maximum is 64% (15, 17). It can be speculated that the reason for the high selectivities obtained from these catalysts is due to all

of the active sites being more energetically similar than in a supported Co/Al_2O_3 catalyst (34). Double bond hydrogenation typically has an activation energy of 3–10 Kcal/mol. For these catalysts this value is between 15–20 Kcal/mol. However, these catalysts have specific activities similar to those for typical catalysts.

Reaction rates calculated from the results shown in Fig. 9 at low conversion are shown in Table 1 for two temperatures. The rates are given per unit mass of active catalyst and can be normalized by the BET surface area to obtain specific rates. It can be seen that the rates for the LT and HT1 catalysts are similar, whereas the rates of the HT2 catalyst are higher. The difference depends on the temperature, at $T = 393$ K the HT2 catalyst is about 10 times more active than the LT and HT1 structures, but at 423 K the difference is less than twofold. This suggests that the sites are more energetically different at the low temperature than at the high temperature. The HT1 catalyst has the highest yield at 423 K because of its higher selectivity even though it has a lower rate than the HT2 catalysts. The trends in reaction rates do not reflect the trends in selectivity due to the difference in activation energies of the various steps involved in the reaction. This is shown in detail by the kinetic analysis presented in the next section. The rates of the Ti_4Co_{12} materials are lower than those of the Co_4Co_{18} clusters previously studied (34, 35). At 393 K, the LT-Co_4Co_{18} structure exhibited a rate of 2.7×10^{-2} mol/h g which is higher than those of any of the Ti_4Co_{12} structures at that temperature. The differences in the activities between the Ti_4Co_{12} and Co_4Co_{18} structures are not surprising since in the former case the structure is diluted by Ti atoms, suggesting that they do not play a direct role in the reaction. Turnover frequencies were not calculated because this requires us to assign an area per active site and, since we do not know what the specific sites are, this number becomes an arbitrary quantity.

An important feature of the Ti_4Co_{12} catalysts is that they show little deactivation during the reaction studied over a 40-h period. Figure 8 shows the 2-butenal conversion, 2-butenol selectivity, and 2-butenol yield as a function of time on stream for the HT1-Ti_4Co_{12} catalyst. After an initial activation period, conversion and selectivity remain relatively constant over a 40-h period. The increase in activity with time on stream has been observed in all our work done with cluster-based catalysts. We speculate that in addition to the fast transient occurring when the reactant is introduced into the reactor, there is a surface transformation induced by the feed that activates the catalysts and forms the selective sites. The 2-butenol conversion decreases slightly from 27 to 24% over the 40-h period. This slight deactivation is probably due to carbon building up on the catalyst surface which blocks the active metal sites. The decrease in 2-butenal conversion is accompanied by a slight increase in 2-butenol selectivity such that the 2-butenol yield remains

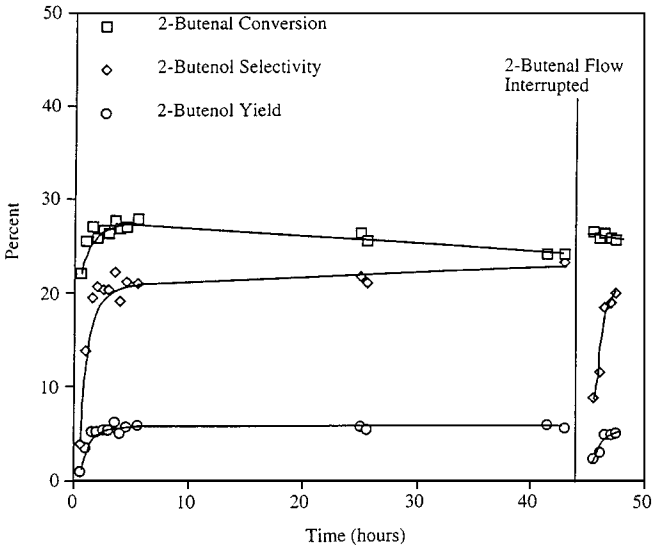

FIG. 8. Long time stability of the HT1-Ti_4Co_{12} catalyst.

constant over the 40 h. At the 44-h mark the 2-butenal flow was interrupted and only the hydrogen was passed over the catalyst. When the 2-butenal flow was restarted 2 h later, the same activation period was seen, with the conversion and selectivity returning to the same previous steady state values. This repetition of the activation period demonstrates that this is a reactant sensitive reaction, where the presence of the reactants and/or products alters the active sites in such a way as to determine the product distribution. Also, it can be seen that the 2-butenal conversion returns to a value of 27%. This adds support to the theory that the decrease in activity is due to carbon deposits on the surface. Because temperature-programmed oxidation was not possible without oxidizing the catalysts and changing their structure, direct measurement of carbon laydown was not conducted. The important result is that the small activity decrease could be regenerated. This implies that the small deactivation observed was not due to structural changes, but rather is due to adsorbed species blocking the surface. Structural changes would be irreversible and the activity could not be recovered with treatment in hydrogen.

Kinetic Modeling

To gain a better understanding of the differences among the various cluster structures in the selectivities of the catalysts for the hydrogenation of 2-butenal, kinetic modeling was attempted to gain an understanding of how the kinetic parameters change, depending on the catalyst structure. The modeling was performed for HT1-Ti_4Co_{12} and HT2-Ti_4Co_{12} only. No modeling was completed for LT-Ti_4Co_{12} since it can only be used at temperatures less than 393 K and reactions were only performed for this structure at the one temperature. There is very limited data in the literature as to preexponential factors and activation energies

TABLE 2

Reaction Steps Used for the Kinetic Model

Adsorption/desorption

$H_2 + 2S \underset{k_{10}}{\overset{k_9}{\rightleftharpoons}} 2H{\bullet}S$

$CH_3CH{=}CHCHO + S \underset{k_{12}}{\overset{k_{11}}{\rightleftharpoons}} CH_3CH{=}CHCHO{\bullet}S$

$CH_3CH{=}CHCH_2OH + S \underset{k_{14}}{\overset{k_{13}}{\rightleftharpoons}} CH_3CH{=}CHCH_2OH{\bullet}S$

$CH_3CH_2CH_2CHO + S \underset{k_{16}}{\overset{k_{15}}{\rightleftharpoons}} CH_3CH_2CH_2CHO{\bullet}S$

$CH_3CH_2CH_2CH_2OH + S \underset{k_{18}}{\overset{k_{17}}{\rightleftharpoons}} CH_3CH_2CH_2CH_2OH{\bullet}S$

$CH_3CH_2CH_2CH_3 + S \underset{k_{20}}{\overset{k_{19}}{\rightleftharpoons}} CH_3CH_2CH_2CH_3{\bullet}S$

Surface reactions

$CH_3CH{=}CHCHO{\bullet}S + 2H{\bullet}S \overset{k_1}{\rightarrow} CH_3CH{=}CHCH_2OH{\bullet}S + 2S$

$CH_3CH{=}CHCHO{\bullet}S + 2H{\bullet}S \overset{k_3}{\rightarrow} CH_3CH_2CH_2CHO{\bullet}S + 2S$

$CH_3CH{=}CHCH_2OH{\bullet}S \overset{k_4}{\rightarrow} CH_3CH_2CH_2COH{\bullet}S$

$CH_3CH{=}CHCH_2OH{\bullet}S + 2H{\bullet}S \overset{k_5}{\rightarrow} CH_3CH_2CH_2CH_2OH{\bullet}S + 2S$

$CH_3CH_2CH_2CHO{\bullet}S + 2H{\bullet}S \overset{k_6}{\rightarrow} CH_3CH_2CH_2CH_2OH{\bullet}S + 2S$

$CH_3CH_2CH_2CH_2OH{\bullet}S + 2H{\bullet}S \overset{k_8}{\rightarrow} CH_3CH_2CH_2CH_3{\bullet}S + H_2O$

for the hydrogenation of 2-butenal. For this reason several steps in the surface reaction sequences were lumped since no information about them is available. Furthermore, additional steps would have increased the number of parameters needed to fit the model to experimental results. The parameters in this work will be chosen to best fit the experimental data.

The reaction pathway assumed in the kinetic analysis can be found schematically in Fig. 1 and in more detail in Table 2. It consists of adsorption desorption steps as well as six surface reactions. The dissociative adsorption of hydrogen was assumed to occur in two sites. While it is possible that the adsorption of the C=C and C=O bonds occur on two sites, the limited amount of experimental data did not allow for discrimination of this type. Hence, all the organic molecules were assumed to adsorb reversibly in a single site. All of the surface reactions are assumed to be irreversible (i.e., no dehydrogenation reactions occur). This is expected to be a valid assumption since the reactions were run in a large excess of hydrogen (approximately at 80 : 1 hydrogen to 2-butenal ratio in the inlet feed). Also, reactions with 2-butenol as the reactant show no 2-butenal formation. The hydrogenation of butanol to butane (Eq. [5]) was modeled as involving two adsorbed hydrogen atoms to form H_2O even though the net amount of hydrogen transferred was zero. The sensitivity to the kinetic expression for this reaction with respect to hydrogen is not very important because the low selectivity to butane, and the small change in hydrogen concentration occurring. Additionally, the total gas flow rate was assumed to be constant along the catalyst bed. This is expected to be a good assumption, since hydrogen is in such excess. Even if all the 2-butenal entering the reactor would be fully hydrogenated, the change in total flow would be approximately −2%. Under the reaction conditions used, the change in total flow is significantly less than this value. The reactor is modeled as a packed bed. The design equation for a packed bed catalytic reactor is

$$\frac{dC_i}{d\tau} = r_i. \qquad [1]$$

This equation gives the concentration of the gas species, *i*, as a function of residence time. To allow for a direct comparison between the model and experiment, Eq. [1] was rearranged so the gas partial pressures are given as a function of residence time.

The individual gas partial pressures and surface coverages throughout the catalyst bed are calculated in a step by step method, where the differential in Eq. [1] is replaced by discrete differences. The step size was chosen to be small enough such that reducing it by a factor of 2 did not effect the computer program integration. The reaction was only considered at steady state, so that the surface coverages do not change with time. Surface coverages are determined from the gas partial pressures by developing a system of equations which set up an equilibrium between the gas partial pressure and the surface coverage at each step in the catalyst bed. This system of algebraic equations is

$$\frac{d\theta_A}{dt} = 0 = -k_1\theta_A\theta_H^2 - k_3\theta_A\theta_H^2 + k_{11}P_A\theta_v - k_{12}\theta_A \qquad [2]$$

$$\frac{d\theta_B}{dt} = 0 = k_1\theta_A\theta_H^2 - k_4\theta_B - k_5\theta_B\theta_H^2 + k_{13}P_B\theta_v - k_{14}\theta_B \qquad [3]$$

$$\frac{d\theta_C}{dt} = 0 = k_3\theta_A\theta_H^2 + k_4\theta_B - k_6\theta_C\theta_H^2 + k_{15}P_C\theta_v - k_{16}\theta_C \qquad [4]$$

$$\frac{d\theta_D}{dt} = 0 = k_5\theta_B\theta_H^2 + k_6\theta_C\theta_H^2 - k_8\theta_D\theta_H^2 + k_{17}P_D\theta_v - k_{18}\theta_D \qquad [5]$$

$$\frac{d\theta_E}{dt} = 0 = k_8\theta_D\theta_H^2 + k_{19}P_E\theta_v - k_{20}\theta_E \qquad [6]$$

$$\frac{d\theta_H}{dt} = 0 = -2k_1\theta_A\theta_H^2 - 2k_3\theta_A\theta_H^2 - 2k_5\theta_B\theta_H^2 - 2k_6\theta_C\theta_H^2 - 2k_8\theta_D\theta_H^2 + 2k_9P_{H_2}\theta_v^2 - 2k_{10}\theta_H^2 \qquad [7]$$

$$0 = \theta_A + \theta_B + \theta_C + \theta_D + \theta_E + \theta_H + \theta_v - 1. \qquad [8]$$

This system of seven equations and seven unknowns (the θ's, where A is 2-butenal, B is 2-butenol, C is butanal, D is butanol, E is butane, H is hydrogen, and v is a vacant site) was solved using a Newton–Rhaphson iteration method,

$$\boldsymbol{\theta}_{n+1} = \boldsymbol{\theta}_n - \mathbf{J}^{-1}\mathbf{g}(\boldsymbol{\theta}_n), \qquad [9]$$

where $\boldsymbol{\theta}_{n+1}$, which is a new estimate of the variables, is

calculated from $\boldsymbol{\theta}_n$, which is the present value of the variables, $\mathbf{g}(\boldsymbol{\theta}_n)$, which is the present value of the equations, and $\mathbf{J}^{-1}$, which is the inverse Jacobian matrix. The values of the Jacobian are evaluated according to

$$J_{ij} = \frac{\partial g_i}{\partial \theta_j}(\boldsymbol{\theta}_n). \qquad [10]$$

By using these equations, the 2-butenal conversion and the various selectivities can be calculated as a function of residence time.

The k's in the above system of equations are defined by the Arrenhius relation,

$$k_i = A_i \exp\left(\frac{-E_{ai}}{RT}\right) \qquad [11]$$

where A is the preexponential factor and E_a is the activation energy. Since there is very limited kinetic data in the literature for the hydrogenation of 2-butenal, the values of the preexponential factors and activation energies were chosen to best fit the experimental data. A lattice search was used to minimize the sum of the squares error between the experimental values and the values predicted by the model. Due to the large number of variables, this minimization was not rigorous. The lattice search was written to incorporate up to four of the kinetic parameters at a time. These parameters were changed simultaneously by incremental amounts to find a combination to minimize the sum of the squares error. By sequentially choosing different combinations of the parameters, values of the parameters which would minimize the sum of the squares error were found for both the HT1 and the HT2 structures of Ti_4Co_{12}.

The kinetic parameters calculated to give the best fit of the experimental data can be found in Table 3. Figures 9a and b show a comparison between the model predictions and *experimental results* for HT1-Ti_4Co_{12} and HT2-Ti_4Co_{12} at 453 K, respectively. The continuous curves are the model predictions and the individual points (indicated by $+$, $*$, $\times$, and o) are the experimental results obtained at different space velocities. The model does a good job in simulating the trends in 2-butenal conversion and the product distributions obtained in the experimental results. This is not surprising given the large number of kinetic constants involved. Nonetheless, the model provides a semiquantitative way of ascertaining the kinetic reasons for the differences in the observed product distribution of the HT1 and HT2 catalysts. Given the lumped nature of the model the agreement with the experimental results is not sufficient to validate the reaction mechanism.

An added benefit of the kinetic model is that reaction conditions can be varied to see how they affect the product distribution without having to do the experiments. To utilize this capability of the model, the reaction temperature was varied in the model to see how the 2-butenol yields change for HT1-Ti_4Co_{12}. The reaction temperature was varied in the range used in the experiments to determine the maximum 2-butenol yield which can be obtained from this catalyst. The results can be seen in Fig. 10. As was expected, due the difference in activation energies for the hydrogenation of 2-butenal to 2-butenol and the hydrogenation of 2-butenal to butanal, lower temperatures favor the formation of 2-butenol. The maximum 2-butenol yield predicted by the model is nearly 18%. The highest yield obtained during experiments was 14.0%. It should be noted that the predicted trends coincide with the experimental results shown in Fig. 7 which were obtained at a different set of conditions than the experimental results used to fit the model.

At this point, it is relevant to analyze whether the parameters determined from the minimization procedure have any physical meaning. First, the activation energies for the hydrogenation of 2-butenal to form 2-butenol and butanal (E_1 and E_3, respectively) reported in the literature for platinum catalysts have values between 3–8 kcal/mol (5). However, previous work with the cluster of clusters catalysts have shown their activation energy to be between 15 and 24 kcal/mol (35). Here the values fall between 12 and 17 kcal/mol, so it seems that the values determined from the minimization are reasonable. Additionally, the activation energy for the hydrogenation of 2-butenal to form 2-butenol is between 3 and 5 kcal/mol less than the activation energy for the hydrogenation of 2-butenal to form butanal. Qualitatively, this is what was expected, as outlined in the reaction results.

TABLE 3

Kinetic Parameters for HT1-Ti_4Co_{12} and HT2-Ti_4Co_{12}

	HT1-Ti_4Co_{12}		HT2-Ti_4Co_{12}	
Reaction	A_i mol/g cat s	E_i kcal/mol	A_i mol/g cat s	E_i kcal/mol
1	1.2×10^4	12.7	1.1×10^5	14.0
3	1.1×10^5	17.3	3.2×10^6	17.0
4	5.1×10^{16}	40.4	5.1×10^{16}	40.4
5	4.6×10^4	21.9	4.4×10^4	22.1
6	3.8×10^{12}	30.0	1.7×10^{15}	35.2
8	5.1×10^{11}	30.0	8.7×10^{12}	32.1
9	1.0×10^1	7.0	1.0×10^1	7.0
10	1.4×10^4	12.8	1.4×10^4	12.8
11	7.3×10^6	19.1	7.3×10^6	19.1
12	1.4×10^{13}	32.9	1.4×10^{13}	32.9
13	5.5×10^2	10.1	5.5×10^2	10.1
14	7.5×10^{10}	29.1	7.5×10^{10}	29.1
15	1.2×10^2	8.0	1.2×10^2	8.0
16	3.0×10^{12}	29.8	3.0×10^{12}	29.8
17	1.3×10^2	10.0	1.3×10^2	10.0
18	6.4×10^{16}	37.3	6.4×10^{16}	37.3
19	8.0×10^3	9.0	8.0×10^3	9.0
20	3.3×10^{14}	34.0	3.3×10^{14}	34.0

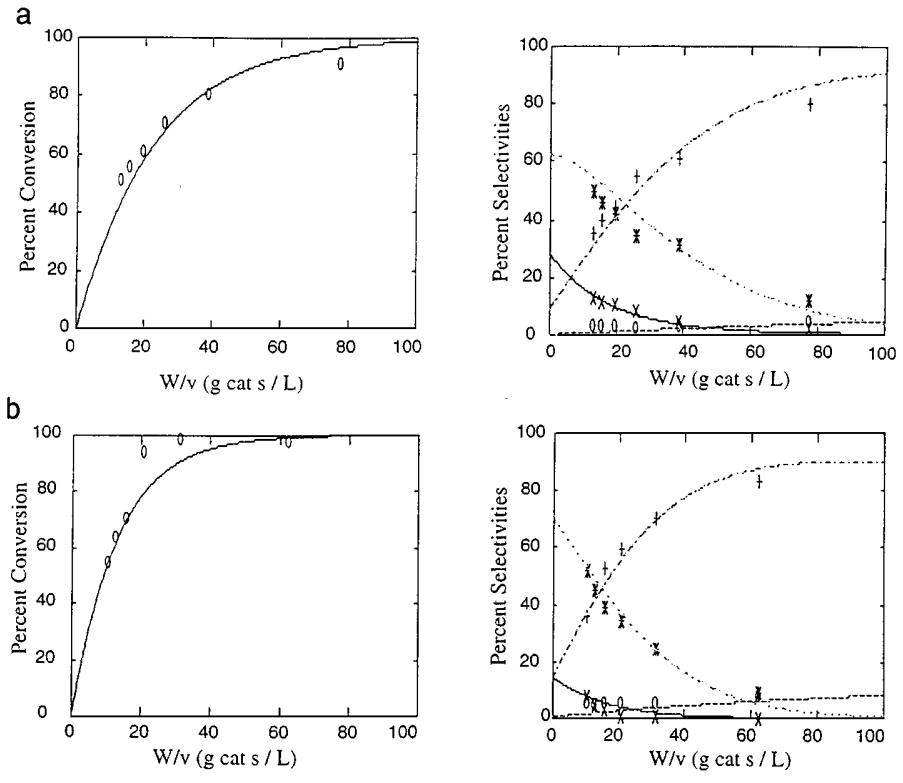

FIG. 9. Comparison of model prediction to experimental values for (a) HT1-Ti_4Co_{12} and (b) HT2-Ti_4Co_{12} (+, butanol; ∗, butanal; ×, 2-butenol; o, butane).

Finally, we can look at the activation energies for the adsorption and desorption of the organic molecules. Subtracting the activation energy of adsorption from the activation energy of desorption gives the heat of adsorption. Typical values of the heat of adsorption of chemisorbed molecules are 20 kcal/mol. Here the values of the heats of adsorption fall in the range of 14 to 27 kcal/mol. So at least to this degree the values of the kinetic parameters of this model seem to be reasonable.

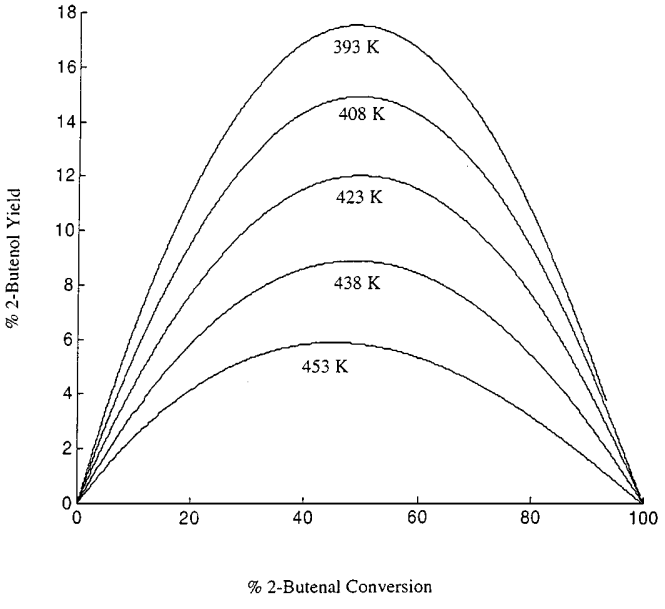

FIG. 10. Model predictions of 2-butenol yields for HT1-Ti_4Co_{12}.

The model evaluates how the kinetic parameters change between the two structures of Ti_4Co_{12}. Here the preexponential factors and activation energies for the adsorption and desorption steps were not changed. The only values varied were the preexponential factors and activation energies for the surface reactions. The most significant changes occur in the values for the hydrogenation of 2-butenal to 2-butenol (A_1, E_1) and the hydrogenation of 2-butenal to butanal (A_3, E_3). The difference in activation energy for the hydrogenation of 2-butenal to form butanal and the hydrogenation of 2-butenal to form 2-butenol for HT1-Ti_4Co_{12} is 4.6 kcal/mol while for HT2-Ti_4Co_{12} this value drops to 3.0 kcal/mol. The larger difference in activation energies for HT1-Ti_4Co_{12} means that using this structure at low temperatures is more beneficial for the formation of 2-butenol than using HT2-Ti_4Co_{12} at low temperatures. Also the ratio $A_1 : A_3$ is higher for HT1-Ti_4Co_{12} (0.11) than it is for HT2-Ti_4Co_{12} (0.03). Larger values for this ratio favor the formation of 2-butenol, the desired product. These two facts explain in kinetic terms the enhanced selectivity to 2-butenol seen with the HT1-Ti_4Co_{12} catalyst.

CONCLUSIONS

The Ti_4Co_{12} cluster of cluster precursor upon thermal activation yields active catalysts for the hydrogenation of 2-butenal. Depending on the activation temperature used, three different catalytic structures can be formed (denoted LT, HT1, and HT2). The hydrogenation of 2-butenal over the Ti_4Co_{12} cluster of cluster catalyst was studied. The catalytic activity of the catalysts depended on the activation temperature. The HT1-Ti_4Co_{12} catalyst was the most successful for the formation of the unsaturated alcohol, 2-butenol. It is speculated that the enhanced production of 2-butenol by the HT1-Ti_4Co_{12} catalyst is due to the presence of a CO_2^- group unique to this structure which would cause increased polarization of the carbonyl group in 2-butenal, facilitating hydrogenation there. The presence of the CO_2^- group in the HT1-Ti_4Co_{12} catalyst was detected during the DRIFTS experiments and confirmed through the temperature-programmed decomposition monitored by mass spectroscopy, which showed CO_2 evolving during the formation of the HT2-Ti_4Co_{12} catalyst.

The maximum 2-butenol yield achieved was 14% while the maximum 2-butenol selectivity achieved was 74%. Kinetic modeling was used to explain in kinetic terms the enhanced selectivity to 2-butenol seen with the HT1-Ti_4Co_{12} catalyst.

ACKNOWLEDGMENTS

This work was partially supported by a Texaco fellowship to the CCRE.

REFERENCES

1. Weissermel, K., and Arpe, H. J., "Industrial Organic Chemistry: Important Raw Materials and Intermediates." Verlag Chemie, New York, 1978.
2. Arctander, S., "Perfume and Flavor Chemicals." Author, Montclair, NJ, 1969.
3. Rylander, P. N., "Catalytic Hydrogenation over Platinum Metals." Academic Press, New York, 1967.
4. Rylander, P. N., "Catalytic Hydrogenation in Organic Syntheses." Academic Press, New York, 1979.
5. Vannice, M. A., and Sen, B., *J. Catal.* **115**, 65 (1989).
6. Bond, G. C., "Catalysis by Metals." Academic Press, New York, 1962.
7. Rylander, P. N., "Hydrogenation Methods." Academic Press, San Diego, CA, 1985.
8. Jenck, J., and Germain, J., *J. Catal.* **65**, 141 (1980).
9. Coloma, F., Sepulveda-Escribano, A., Fierro, J. L. G., and Rodriguez-Reinoso, F., *Appl. Catal. A: General* **136**, 231 (1996).
10. Marinelli, T. B. L., Nabuurs, S., and Ponec, V., *J. Catal.* **151**, 431 (1995).
11. Simonik, J., and Beranek, L., *Coll. Czech. Chem. Commun.* **37**, 353 (1972).
12. Raab, C. G., and Lercher, J. A., *J. Mol. Catal.* **75**, 71 (1992).
13. Noller, H., and Lin, W. M., *J. Catal.* **85**, 25 (1984).
14. Lawrence, S. S., and Schreifels, J. A., *J. Catal.* **119**, 272 (1989).
15. Hutchings, G. J., King, F., Okoye, I. P., and Rochester, C. H., *Appl. Catal. A: General* **83**, L7 (1992).
16. Hutchings, G., King, F., Okoye, I., and Rochester, C., *Catal. Lett.* **23**, 127 (1994).
17. Englisch, M., Jentys, A., and Lercher, J. A., *J. Catal.* **166**, 25 (1997).
18. Coloma, F., Sepulveda-Escribano, A., Fierro, J. L. G., and Rodriguez-Reinoso, F., *Appl. Catal. A: General* **150**, 165 (1997).
19. Raab, C. G., Englisch, M., Marinelli, T. B. L. W., and Lercher, J. A., *in* "Heterogeneous Catalysis and Fine Chemicals II" (M. Guisnet *et al.*, Eds.), Vol. 78, p. 211. Elsevier Science, Amsterdam, 1993.
20. Makouangou-Mandilou, R., Touroude, R., and Dauscher, A., *in* "Heterogeneous Catalysis and Fine Chemicals II" (M. Guisnet *et al.*, Eds.), Vol. 78, p. 219. Elsevier Science, Amsterdam, 1993.
21. Hubaut, R., Daage, M., and Bonnelle, J. P., *Appl. Catal.* **22**, 231 (1986).
22. Raab, C. G., and Lercher, J. A., *Catal. Lett.* **18**, 99 (1993).
23. Makouangou, R., Dauscher, A., and Touroude, R., *in* "New Frontiers in Catalysis" (L. Guczi, F. Solymosi, and P. Tetenyi, Eds.), Vol. 75c, p. 2475. Elsevier, Amsterdam, 1993.
24. Beccat, P., Bertolini, J. C., Gauthier, Y., Massardier, J., and Ruiz, P., *J. Catal.* **126**, 451 (1990).
25. Nashner, M. S., *et al.*, *J. Am. Chem. Soc.* **118**, 12964 (1996).
26. Gates, B. C., *Chem. Rev.* **95**, 511–522 (1995).
27. Ichikawa, M., *in* "Tailored Metal Catalysts" (Y. Iwasawa, Ed.), p. 183. Reidel, Boston, 1986.
28. Lewis, L. N., *Chem. Rev.* **93**, 2693 (1993).
29. Cen, W., Haller, K. J., and Fehlner, T. P., *Inorg. Chem.* **30**, 3120 (1991).
30. Cen, W., Haller, K. J., and Fehlner, T. P., *Inorg. Chem.* **31**, 2672 (1992).
31. Cen, W., Haller, K. J., and Fehlner, T. P., *Inorg. Chem.* **32**, 995 (1993).
32. Bañares, M., Patil, A. N., Fehlner, T. P., and Wolf, E. E., *Catal. Lett.* **34**, 251 (1995).
33. Bañares, M., *et al.*, *Chem. Mat.* **7**, 553 (1995).
34. Bañares, M. A., Dauphin, L., Calvo-Pérez, V., Fehlner, T. P., and Wolf, E. E., *J. Catal.* **152**, 396 (1995).
35. Patil, A. N., Bañares, M. A., Lei, X., Fehlner, T. P., and Wolf, E. E., *J. Catal.* **159**, 458 (1996).
36. Lei, X., Shang, M., and Fehlenr, T. P., *Organometallics* **15**, 3779 (1996).
37. Socrates, G., "Infrared Characteristic Group Frequencies," Wiley, New York, 1980.
38. Cen, W., Ladna, B., Fehlner, T. P., Miller, A. E., and Yue, D., *J. Organometallic Chem.* **449**, 19 (1993).